ISSN 0016-7029, Geochemistry International, 2007, Vol. 45, No. 6, pp. 569–579. © Pleiades Publishing, Ltd., 2007.
Original Russian Text © N.V. Surkov, Yu.G. Gartvich, O.P. Izokh, 2007, published in Geokhimiya, 2007, No. 6, pp. 632–642.

Stability and Phase Relations of Nonstoichiometric Clinopyroxenes in the Join Diopside–Ca-Eskola Component at High Pressures

N. V. Surkov, Yu. G. Gartvich, and O. P. Izokh

Institute of Mineralogy and Petrography, Siberian Division, Russian Academy of Sciences, pr. Akademika Koptyuga 3, Novosibirsk, 630090 Russia

e-mail: diagrams@uiggm.nsc.ru

Received December 15, 2005

Abstract—The stability of nonstoichiometric clinopyroxenes in the Di–CaEsk join was experimentally studied, and phase diagrams were constructed for this join at pressures of 2.0 and 3.0 GPa. It was found that melting in the diopside part of the join occurs at anomalously low temperatures, and nonstoichiometric clinopyroxene coexists with a phase approaching diopside in composition. Phase relations along the Di–CaEsk join can be described and consistently interpreted only assuming that the diopside phase (α-diopside) is thermodynamically stable. The following phase volumes were observed along the solidus of the join at a pressure of 3.0 GPa: *Cpx*, α*Di* + *Cpx*, α*Di* + *Cpx* + *Qtz*, α*Di* + *Cpx* + *Grt* + *Qtz*, *Cpx* + *Grt* + *Qtz*, *Cpx* + *Grt* + *Ky* + *Qtz*, *Grt* + *Ky* + *Qtz*. Melting occurs via the eutectic reaction α*Di* + *Cpx* + *Grt* + *Qtz* = *L* at a temperature of about 1200°C in the diopside part of the system and via the eutectic reaction *Cpx* + *Grt* + *Ky* + *Qtz* = *L* at a temperature of 1400°C in the calcium-rich part of the system. At a pressure of 2.0 GPa, melting occurs at temperatures of 1200–1300°C via the eutectic reaction α*Di* + *Cpx* + An + Qtz = *L*. The invariant equilibrium (*L*, *An*, *Cpx*, *Grt*, α*Di*, *Qtz*) lies within the pressure range 2.0–3.0 GPa. Nonstoichiometric clinopyroxenes form complex solid solutions, the compositions of which are not strictly confined to the Di–CaEsk join and depend on temperature, pressure, and phase association. Grossular garnets coexist with nonstoichiometric clinopyroxenes and α-diopside.

DOI: 10.1134/S0016702907060055

INTRODUCTION

The compositions of natural clinopyroxenes can usually be described in terms of stoichiometric end-members. Deviations from stoichiometry in their compositions are rare and difficult to identify. Nonetheless, significant amounts of excess silica were detected in clinopyroxenes from kyanite eclogites and grospydite xenoliths. High-alumina omphacites from grospydites show a significant cation deficit, and oriented acicular inclusions of quartz and plagioclase were described in eclogitic clinopyroxenes [1].

The presence of excess silica is attributed to the incorporation of a jadeite-like end-member, $Ca_{0.5}AlSi_2O_6$, the existence of which was supposed by Eskola [2]. Nonstoichiometric clinopyroxenes were first experimentally synthesized and studied by Kushiro [3]. Systematic experimental studies of nonstoichiometric clinopyroxenes were undertaken after the investigation of melting of calc-alkaline rocks had established the absence of free quartz during the crystallization of clinopyroxene-bearing associations in the field of quartz-normative compositions [4–6].

Based on the results of high-pressure experiments with synthetic compositions of the systems $CaMgSi_2O_6$–$CaAl_2SiO_6$–SiO_2 and $CaMgSi_2O_6$–$NaAlSi_2O_6$–$CaAl_2SiO_6$–SiO_2 [7–13], it was supposed that excess silica can be dissolved in clinopyroxene as a jadeite-like end-member, $Ca_{0.5}AlSi_2O_6$, which was referred to as the Ca-Eskola molecule (CaEsk). The maximum extension of solid solutions toward the Ca-Eskola molecule was observed in the ternary join $CaMgSi_2O_6$–$CaAl_2SiO_6$–$Ca_{0.5}AlSi_2O_6$. Other authors [14] also demonstrated a relation between the contents of alumina and excess SiO_2.

Proceeding from the suggestion on the possible use of the Ca-Eskola component as a pressure indicator, attempts to calibrate the dependence of the composition of nonstoichiometric clinopyroxene on temperature and pressure were undertaken on the basis of both experimental data and thermodynamic calculations [12, 13, 15–18]. A comparison of published data reveals severe contradictions both in the extent of solid solutions and the character of assemblages of nonstoichiometric clinopyroxenes. The analysis of all available data suggests that the solution of the problem of nonstoichiometric clinopyroxene stability requires a revision on the basis of a comprehensive experimental study.

Our reconnaissance study [18] showed that phase relations in the join $CaMgSi_2O_6$–$Ca_{0.5}AlSi_2O_6$ at 3.0 GPa are significantly different from those expected from the interpolation of the data of previous studies. A new previously unidentified phase was discovered in this join.

Table 1. Characteristics of starting materials

Starting material			Treatment conditions	Phase association
Name	Components			
	Di	CaEsk		
	mol %	mol %		
S33	100	0	P = 1 atm, T = 1500°C, 0.5 h, 1300°C 6 h	diopside
S30	0	100	P = 1 atm, T = 1500°C, 0.5 h, 1150°C 6 h	subsolidus phases
S118	90	10	P = 1 atm, T = 1150°C, 48 h	subsolidus phases
S71	80	20	P = 1 atm, T = 1150°C, 48 h	subsolidus phases
S71a	80	20	P = 1 atm, T = 1150°C, 48 h, T = 1600°C, 0.5 h	glass
S115	70	30	P = 1 atm, T = 1150°C, 48 h	subsolidus phases
S114	50	50	P = 1 atm, T = 1150°C, 48 h	subsolidus phases
S114a	50	50	P = 1 atm, T = 1150°C, 48 h, T = 1600°C, 0.5 h	glass
S120	30	70	P = 1 atm, T = 1150°C, 48 h	subsolidus phases

Its composition approaches that of diopside and is free of alumina (referred to as α-diopside, α*Di*). The appearance of α-diopside results in the formation of new univariant equilibria with this phase, including eutectic ones, which leads to a sharp decrease in the temperature of melt appearance in the join $CaMgSi_2O_6$–$Ca_{0.5}AlSi_2O_6$.

In order to solve problems arising from the reevaluation of phase relations in the join $CaMgSi_2O_6$–$Ca_{0.5}AlSi_2O_6$ indicating the stability of the new phase (α-diopside) and nonstoichiometric clinopyroxene solid solutions, the phase diagram of the Di–CaEsk join was experimentally investigated in detail at pressures of 2.0–3.0 GPa. Experiments were carried out on a high-pressure piston-cylinder apparatus by the quench technique using procedures similar to those described by other researchers [19–22].

Heated and pressed sodium chloride was used as a pressure medium in the cell assembly [23], which allowed precise control of pressure and completely excluded the presence of volatile components, such as water or hydrogen. Pressure and temperature were controlled during experiments with precisions of + 0.03 GPa and ±1°C, respectively. The accuracy of temperature measurement was better than ±5°C.

Stoichiometric starting mixtures corresponding to diopside ($CaMgSi_2O_6$) and Ca-Eskola molecule ($Ca_{0.5}AlSi_2O_6$) were prepared by the weight method from annealed high-purity reagents. These mixtures were heated at temperatures of 1100–1300°C under atmospheric pressure for 8–10 h, pulverized in a hard-facing alloy mortar, and again heated until the complete disappearance of the initial oxides. Working mixtures of intermediate compositions along the join diopside–Ca-Eskola component were prepared from the above compounds. One part of them was fused into a transparent glass in a platinum crucible at temperatures of 1500–1600°C, and the remaining part was annealed at 1100–1200°C and consisted of mixed subsolidus phases (Table 1).

The choice of equilibrium criteria is a major challenge in experimental studies. It was previously shown [24] that the method of equilibrium approach from two directions is insufficient for the substantiation of the attainment of equilibrium in phase assemblages including multicomponent solid solutions. More compelling evidence for the attainment of equilibrium can be provided by identical results in experiments with starting material of different characters (for instance, phase associations) coupled with negligible changes in experimental results in response to a substantial increase in run duration. In such a case, the attainment of equilibrium in experiments is ensured by using long run durations, definitely in excess of those necessary to provide time-invariant results [25].

The experimental working mixture was loaded into a platinum capsule, annealed at 500–600°C for 7–8 h, and sealed by arc welding. After the experiment, a double-polished thin section oriented parallel the vertical axis of the capsule was prepared from each sample. Phases were identified using an optical microscope and X-ray phase analysis on a Dron-3 diffractometer. The compositions of phases were determined using a Camebax-Micro electron microprobe. Zoning within grains and compositional variations between grains were never observed. Melting was reliably detected from the presence of glass during the examination of thin sections. Glass was well preserved in experimental samples and quench phases were never observed.

The results of experiments are given in Table 2. The electron microprobe analyses of phases are shown in Table 3. Phase relation established in the 3.0 GPa experiments are somewhat different from those that could have been expected from the extrapolation of the

Table 2. Results of experiments in the join $CaMgSi_2O_6$–$Ca_{0.5}AlSi_2O_6$

Run no.	*P*, GPa	*T*, °C	Duration, h	Starting material no.	Content of $Ca_{0.5}AlSi_2O_6$ in starting material, mol %	Identified phases
P454	3.0	1505	0.3	S118	10	α*Di* + *Cpx* + *L*
P457	3.0	1428	5	S118	10	α*Di* + *Cpx* + *L*+*Qtz*
P459	3.0	1408	7	S118	10	α*Di* + *Cpx* + *Qtz*
P42	3.0	1511	3	S71	20	α*Di* + *Cpx* + *L*
P45	3.0	1456	5	S71	20	α*Di* + *Grt* + *L*+*Cpx*
P48	3.0	1412	6	S71a	20	α*Di* + *Cpx* + *Grt* + *L*
P56	3.0	1358	6	S71	20	α*Di* + *Grt* + *Cpx* + *L*
P451	3.0	1530	3	S115	30	α*Di* + *Cpx* + *L*
P448	3.0	1507	3	S115	30	α*Di* + *Cpx* + *L*
P439	3.0	1407	8	S115	30	α*Di* + *Cpx* + *L*+*Grt*
P442	3.0	1306	18	S115	30	α*Di* + *Cpx* + *L*+*Grt*
P445	3.0	1208	38	S115	30	α*Di* + *Cpx* + *Grt* + *Qtz*
P450	3.0	1530	3	S114	50	*Cpx* + *L*
P447	3.0	1507	3	S114	50	*Cpx* + *L*
P458	3.0	1428	5	S114	50	*Cpx* + *L*+*Grt*
P438	3.0	1407	8	S114a	50	*Cpx* + *Grt* + *L*
P441	3.0	1306	18	S114	50	*Cpx* + *Grt* + *Qtz*
P444	3.0	1208	38	S114	50	*Cpx* + *Grt* + *Qtz* + *Ky*
P461	3.0	1408	7	S120	70	*Cpx* + *L*
P474	2.0	1456	5.5	S71	20	α*Di* + *L*+*Cpx*
P462	2.0	1403	6.5	S71	20	α*Di* + *Cpx* + *L*
P471	2.0	1354	9.5	S71	20	α*Di* + *Cpx* + *L*
P465	2.0	1297	16.5	S71	20	α*Di* + *Cpx* + *L*
P469	2.0	1207	38	S71a	20	α*Di* + *Qtz* + *An* + *Cpx*
P476	2.0	1456	5.5	S115	30	*L*
P463	2.0	1404	6.5	S115	30	α*Di* + *Cpx* + *L*
P472	2.0	1354	9.5	S115	30	α*Di* + *Cpx* + *L*
P467	2.0	1297	16.5	S115	30	*Cpx* + *L*+α*Di*
P468	2.0	1207	38	S115	30	α*Di* + *Qtz* + *An*
P475	2.0	1456	5.5	S114	50	*L*
P464	2.0	1403	6.5	S114	50	α*Di* + *Cpx* + *L*
P473	2.0	1354	9.5	S114	50	α*Di* + *Cpx* + *L*
P466	2.0	1297	16.5	S114	50	α*Di* + *Cpx* + *L*
P470	2.0	1207	38	S114	50	α*Di* + *Qtz* + *An* + *Cpx*

available data. In the calcium-rich part of the system (more than 50 mol % $Ca_{0.5}AlSi_2O_6$), the observed assemblages (*Cpx* + *Grt* + *Qtz* and *Cpx* + *Grt* + *Ky* + *Qtz*) are in agreement with those expected from the extrapolation of previous data obtained at higher pressures (3.5 GPa) [7–10]. In contrast, near the diopside end of the join, melting at anomalously low temperatures (below 1300°C) was observed instead of the expected field of monomineralic clinopyroxene solid solutions. Glass, garnet, quartz, and nonstoichiometric clinopyroxene were always accompanied by large clinopyroxene crystals (several times larger than the grains of other phases), whose microprobe analyses approached the diopside composition.

The X-ray phase analysis of the samples revealed the presence of two clinopyroxenes. The similarity of

Table 3. Compositions of phases from experiments in the join $CaMgSi_2O_6$–$Ca_{0.5}AlSi_2O_6$

Run no.	Phase	Composition, wt %					Structural formula					Number of analyses
		CaO	MgO	Al_2O_3	SiO_2	Total	Ca	Mg	Al	Si	Total	
1	2	3	4	5	6	7	8	9	10	11	12	13
P454	*Cpx*	22.38	6.38	10.50	62.94	102.2	0.8088	0.3206	0.4174	2.1221	3.669	4
P454	α*Di*	24.62	19.91	0.03	55.89	100.4	0.9429	1.0605	0.0014	1.9971	4.002	4
P457	*Cpx*	23.16	9.65	6.99	60.23	100.0	0.8661	0.5024	0.2870	2.1003	3.756	3
P457	α*Di*	24.84	19.50	0.08	56.21	100.6	0.9493	1.0369	0.0034	2.0042	3.994	6
P459	*Cpx*	23.68	1.39	14.36	60.85	100.3	0.8722	0.0715	0.5819	2.0916	3.617	3
P459	α*Di*	25.98	18.81	0.23	55.15	100.1	1.0024	1.0101	0.0101	1.9861	4.008	2
P42	*L*	20.63	3.77	12.92	63.65	100.9	0.7458	0.1899	0.5138	2.1466	3.596	10
P42	*Cpx*	24.60	16.27	5.28	54.15	100.3	0.9401	0.8650	0.2220	1.9309	3.958	4
P42	α*Di*	25.04	19.15	0.00	56.37	100.5	0.9577	1.0190	0.0000	2.0116	3.988	3
P45	*Gr*	24.67	8.46	24.55	42.32	100.0	1.8984	0.9064	2.0778	3.0391	7.9218	3
P45	*L*	20.29	1.68	19.54	57.23	98.7	0.7530	0.0868	0.7978	1.9816	3.619	2
P45	α*Di*	25.44	18.71	0.04	54.72	98.9	0.9931	1.0162	0.0021	1.9937	4.005	1
P48	*L*	21.33	2.30	15.26	60.79	99.6	0.7841	0.1178	0.6173	2.0860	3.605	2
P48	*Cpx*	23.57	11.67	11.63	51.40	98.2	0.9125	0.6291	0.4958	1.8572	3.894	4
P48	α*Di*	25.71	18.86	0.01	56.18	100.7	0.9835	1.0039	0.0004	2.0059	3.993	1
P56	*Cpx*	22.18	4.21	28.53	44.98	99.9	0.8368	0.2211	1.1842	1.5828	3.825	3
P56	*Grt*	34.15	2.31	21.80	42.01	100.2	2.7003	0.2550	1.8966	3.0998	7.9518	3
P56	α*Di*	24.82	19.58	0.002	55.44	99.8	0.9573	1.0510	0.0001	1.9957	4.004	4
P451	*L*	22.68	6.36	12.03	59.56	100.6	0.8371	0.3265	0.4885	2.0517	3.703	4
P451	*Cpx*	24.53	16.46	4.09	55.20	100.2	0.9362	0.8739	0.1719	1.9659	3.948	2
P451	α*Di*	24.41	19.15	0.00	55.72	99.2	0.9443	1.0311	0.0000	2.0122	3.987	2
P448	*L*	20.40	4.73	12.89	57.62	95.6	0.7855	0.2534	0.5460	2.0709	3.656	1
P448	*Cpx*	23.41	15.91	4.60	50.32	94.2	0.9550	0.9031	0.2064	1.9160	3.980	1
P448	α*Di*	22.87	17.52	0.02	51.85	92.2	0.9524	1.0151	0.0011	2.0153	3.984	1
P439	*L*	22.66	3.45	14.08	59.69	99.8	0.8385	0.1779	0.5733	2.0617	3.651	2
P439	*Cpx*	24.97	16.04	5.93	53.44	100.3	0.9554	0.8535	0.2498	1.9081	3.966	3
P439	α*Di*	24.91	18.21	0.10	55.13	98.3	0.9747	0.9916	0.0046	2.0133	3.984	3
P442	*L*	22.69	3.25	12.81	61.38	100.1	0.8355	0.1665	0.5189	2.1097	3.630	1
P442	*Cpx*	24.79	14.60	6.98	53.36	99.7	0.9522	0.7805	0.2950	1.9123	3.940	4
P442	α*Di*	24.89	19.30	0.00	55.52	99.7	0.9611	1.0369	0.0000	2.0009	3.999	1
P445	*Gr*	29.69	3.26	24.43	40.54	97.9	2.3718	0.3623	2.1468	3.0227	7.9038	1
P445	*Cpx*	24.75	14.82	14.73	46.20	100.5	0.9543	0.7912	0.6232	1.6597	4.028	2
P445	α*Di*	25.18	19.07	0.03	56.23	100.5	0.9641	1.0158	0.0012	2.0090	3.990	4
P450	*L*	19.12	7.80	15.01	59.97	101.9	0.6883	0.3907	0.5942	2.0147	3.688	7
P450	*Cpx*	23.50	15.37	7.52	52.95	99.3	0.9031	0.8216	0.3180	1.8990	3.941	3
P450	α*Di*	25.26	19.38	0.065	5.53	100.2	0.9715	1.0371	0.0028	1.9934	4.005	1
P447	*L*	17.99	5.54	15.69	60.94	100.1	0.6529	0.2798	0.6264	2.0638	3.622	6
P447	*Cpx*	23.38	14.86	8.92	52.48	99.6	0.8951	0.7916	0.3758	1.8747	3.937	7
P458	*L*	19.21	7.58	15.70	59.85	102.3	0.6885	0.3780	0.6192	2.0022	3.688	3
P458	*Cpx*	23.63	15.82	8.40	52.06	99.9	0.9050	0.8429	0.3537	1.8606	3.962	3
P438	*L*	17.70	5.54	16.48	61.46	101.1	0.6347	0.2763	0.6500	2.0569	3.618	4
P438	*Cpx*	23.61	14.55	10.12	51.28	99.5	0.9065	0.7775	0.4272	1.8374	3.948	3

Table 3. (Contd.)

Run no.	Phase	Composition, wt %					Structural formula					Number of analyses
		CaO	MgO	Al_2O_3	SiO_2	Total	Ca	Mg	Al	Si	Total	
1	2	3	4	5	6	7	8	9	10	11	12	13
P441	*Cpx*	23.51	14.60	9.67	51.97	99.7	0.8997	0.7774	0.4069	1.8561	3.940	4
P444	*Grt*	32.03	3.90	22.81	41.11	99.8	2.5310	0.4289	1.9834	3.0324	7.9758	2
P444	*Cpx*	24.54	13.71	11.66	49.84	99.7	0.9447	0.7344	0.4938	1.7900	3.963	4
P461	*Cpx*	22.97	7.96	22.81	46.32	100.0	0.8713	0.4204	0.9517	1.6402	3.883	4
P474	*L*	20.46	6.72	12.19	61.35	100.7	0.7465	0.3416	0.4892	2.0889	3.666	7
P474	α*Di*	24.16	20.25	0.04	55.43	99.9	0.9300	1.0847	0.0017	1.9912	4.007	3
P462	*L*	20.69	3.84	15.20	61.77	101.5	0.7461	0.1927	0.6028	2.0784	3.620	4
P462	*Cpx*	25.08	16.33	5.14	54.02	100.5	0.9575	0.8677	0.2163	1.9250	3.966	3
P462	α*Di*	25.15	19.36	0.01	55.75	100.2	0.9661	1.0350	0.0007	1.9988	4.000	2
P471	*L*	22.07	2.15	15.93	60.83	100.9	0.8032	0.1088	0.6375	2.0657	3.615	3
P471	*Cpx*	24.12	12.95	12.87	50.64	100.6	0.9166	0.6855	0.5372	1.7959	3.935	2
P471	α*Di*	24.06	20.21	0.02	56.25	100.5	0.9181	1.0731	0.0010	2.0035	3.995	1
P465	*L*	20.92	6.94	11.36	62.01	101.2	0.7605	0.3511	0.4541	2.1035	3.669	2
P465	*Cpx*	24.93	17.84	2.96	54.05	99.7	0.9619	0.9575	0.1258	1.9458	3.991	3
P465	α*Di*	24.26	20.15	0.03	56.17	100.6	0.9261	1.0700	0.0013	2.0009	3.998	2
P469	α*Di*	24.73	19.74	0.06	56.58	101.1	0.9395	1.0435	0.0028	2.0063	3.992	5
P476	*L*	27.87	18.96	9.44	44.95	101.2	1.0875	1.0296	0.4054	1.6373	4.159	3
P463	*L*	21.63	4.30	14.29	60.64	100.8	0.7895	0.2184	0.5738	2.0655	3.647	3
P463	*Cpx*	24.83	16.05	6.56	51.94	99.3	0.9617	0.8644	0.2800	1.8768	3.983	2
P463	α*Di*	24.94	19.37	0.02	55.89	100.2	0.9578	1.0349	0.0011	2.0027	3.996	3
P472	*L*	23.09	2.20	14.87	60.87	101.0	0.8431	0.1117	0.5973	2.0745	3.626	2
P472	*Cpx*	25.23	16.77	4.63	53.27	99.9	0.9724	0.8997	0.1964	1.9165	3.985	5
P472	α*Di*	24.57	19.78	0.04	55.71	100.1	0.9442	1.0575	0.0016	1.9978	4.001	2
P467	*L*	21.99	4.88	14.25	60.24	101.3	0.8011	0.2470	0.5711	2.0475	3.666	3
P467	*Cpx*	25.23	16.62	6.04	52.29	100.2	0.9707	0.8899	0.2559	1.8777	3.994	6
P468	α*Di*	25.47	19.64	0.02	56.90	102.0	0.9607	1.0309	0.0011	2.0033	3.996	3
P464	*L*	18.72	6.18	15.78	61.06	101.7	0.6712	0.3083	0.6224	2.0433	3.645	4
P464	*Cpx*	24.20	16.10	7.42	52.53	100.2	0.9255	0.8568	0.3121	1.8747	3.969	4
P464	α*Di*	25.26	19.81	0.16	55.57	100.8	0.9664	1.0546	0.0067	1.9844	4.012	1
P473	*L*	16.44	3.50	17.68	61.96	99.6	0.5936	0.1762	0.7022	2.0883	3.560	2
P473	*Cpx*	23.21	12.75	12.77	50.75	99.4	0.8885	0.6793	0.5375	1.8129	3.918	5
P473	α*Di*	25.19	19.13	0.01	56.10	100.4	0.9653	1.0200	0.0005	2.0068	3.992	2
P466	*L*	18.99	7.14	15.28	60.57	101.9	0.6813	0.3566	0.6032	2.0285	3.669	3
P466	*Cpx*	24.39	16.80	6.02	53.47	100.6	0.9291	0.8906	0.2524	1.9007	3.973	5
P466	α*Di*	24.61	19.85	0.05	55.74	100.2	0.9442	1.0597	0.0023	1.9961	4.002	1
P470	α*Di*	24.68	18.89	0.25	54.26	98.0	0.9703	1.0321	0.0110	1.9904	4.004	2

Note: The structural formulae were calculated on the basis of 6 oxygen atoms for glasses, α-diopside, and clinopyroxene and 12 O atoms for garnet.

their structural characteristics complicates their simultaneous identification. The X-ray structural investigation of diopside-rich (90 mol %) samples showed that the structure of the dominant clinopyroxene from the experimental products is not different at atmospheric pressure and room temperature from that of the previously studied samples of synthetic diopside [26, 27].

When pressure decreased to 2.0 GPa, assemblages including clinopyroxene, diopside, anorthite, and quartz were formed in the join. Melting was again observed at anomalously low temperatures.

The established phase relations cannot be explained on the basis of previous concepts on possible phase associations involving nonstoichiometric clinopyroxene, pyrope–grossular garnet, anorthite, quartz, kyanite (sillimanite), and liquid. The anomalously low melting temperatures of the compositions are especially difficult to explain. The occurrence of melting at temperatures much lower than the temperatures of eutectics involving the aforementioned phases of the system studied implies the appearance of a new eutectic point, which, in turn, requires the formation of an additional phase. This role can probably belong to the phase of diopside composition detected in the experimental products. Since this phase was formed both near the liquidus and below the solidus, was detected in the products of experiments with starting glasses and subsolidus crystalline phases (1 atm), and did not disappear at experimental durations definitely exceeding the time necessary for equilibration, the metastable formation and existence of this phase are unlikely. Furthermore, the grains of the diopside phase are always several times larger than the grains of other phases, nonstoichiometric clinopyroxene, garnet, anorthite, and quartz. Such relationships of grain sizes are certainly at odds with the suggestion on the metastable formation or existence of the diopside phase. Thus, it can be concluded that the diopside phase is stable in the assemblages of the join diopside–Ca-Eskola molecule.

In this connection, some characteristic features of the diopside phase should be pointed out. Its composition is peculiar in that it is devoid of alumina and matches almost perfectly the stoichiometry of diopside. The admixture of the enstatite component is no higher than 5 mol %. Optical examination of thin sections showed that the diopside phase occurs as grains showing rhombic cross-section normal to the elongation and irregular columnar cross-sections parallel to the elongation [18]. All the grains of this phase exhibit fine polysynthetic twinning parallel to the elongation and coarser twinning normal to the elongation. The twins can be recognized only in double-polished sections and at high magnifications. The character of the twinning allows us to suppose that the diopside phase had a different structure at high temperatures and underwent a polymorphic transition during a decrease in temperature and pressure.

The suggestion of a polymorphic transition in the diopside phase seems to be reasonable, especially taking into account that diopsidic clinopyroxene forms a continuous series of solid solutions toward the aluminous component [28]. Therefore, the coexistence of nonstoichiometric aluminous clinopyroxene and aluminum-free diopside is unlikely. Thus, it can be suggested that the diopside phase detected in the experimental products does not quench at decreasing temperature and transforms into a phase with the most similar composition, i.e., diopside. The consequences of this transition are reflected in polysynthetic twinning. Because of this, the diopside phase is hereafter referred to as α-diopside. The structural characteristics of α-diopside must be determined at high temperatures (about 1200°C) and pressures, which is the subject of a future study.

The suggestion on the existence of the independent α-diopside phase different from the clinopyroxene solid solution allows us to reconcile the phase diagram of the join diopside–Ca-Eskola molecule ($CaMgSi_2O_6$–$CaAl_{0.5}Si_2O_6$) with the phase rule. In addition to the above arguments, this result provides direct thermodynamic support for the existence of the α-diopside phase.

The above considerations allow us to propose a variant of the phase diagram of the join diopside–Ca-Eskola molecule, which shows the following characteristics (Figs. 1–3). The melting temperature of diopside clinopyroxene is given according to the data of Boyd and England [29], and phase relations at the Ca-Eskola side of the diagram are shown on the basis of the Surkov and Doroshev [30] data.

At a pressure of 3.0 GPa, the following sequence of phase volumes is observed along the solidus of the system in the direction from diopside to the Ca-Eskola component: *Cpx*, α*Di* + *Cpx*, α*Di* + *Cpx* + *Qtz*, α*Di* + *Cpx* + *Grt* + *Qtz*, *Cpx* + *Grt* + *Qtz*, *Cpx* + *Grt* + *Ky* + *Qtz,* and *Grt* + *Ky* + *Qtz.* In the liquidus region of the diopside part of the join, melting occurs at temperatures of higher than 1200°C via the eutectic reaction α*Di* + *Cpx* + *Grt* + *Qtz* = *L,* whereas in the calcium-rich part of the system, the eutectic melting reaction *Cpx* + *Grt* + *Ky* + *Qtz* = *L* occurs at a temperature of slightly higher than 1400°C. Nonstoichiometric clinopyroxene forms limited solid solutions containing up to 23 mol % of the Ca-Eskola end-member. The content of $Ca_{0.5}AlSi_2O_6$ in clinopyroxene increases with decreasing temperature and depends on the phase assemblage. The compositions of clinopyroxene solid solutions coexisting with liquid at high temperatures cannot be expressed in terms of ordinary pyroxene end-members, whereas the clinopyroxenes from most other experiments are represented by four-component solid solutions $Mg_2Si_2O_6$–$CaMgSi_2O_6$–$CaAl_2SiO_6$–$Ca_{0.5}AlSi_2O_6$. Garnets coexisting with the nonstoichiometric clinopyroxenes have grossular-rich compositions with no more than 32 mol % pyrope.

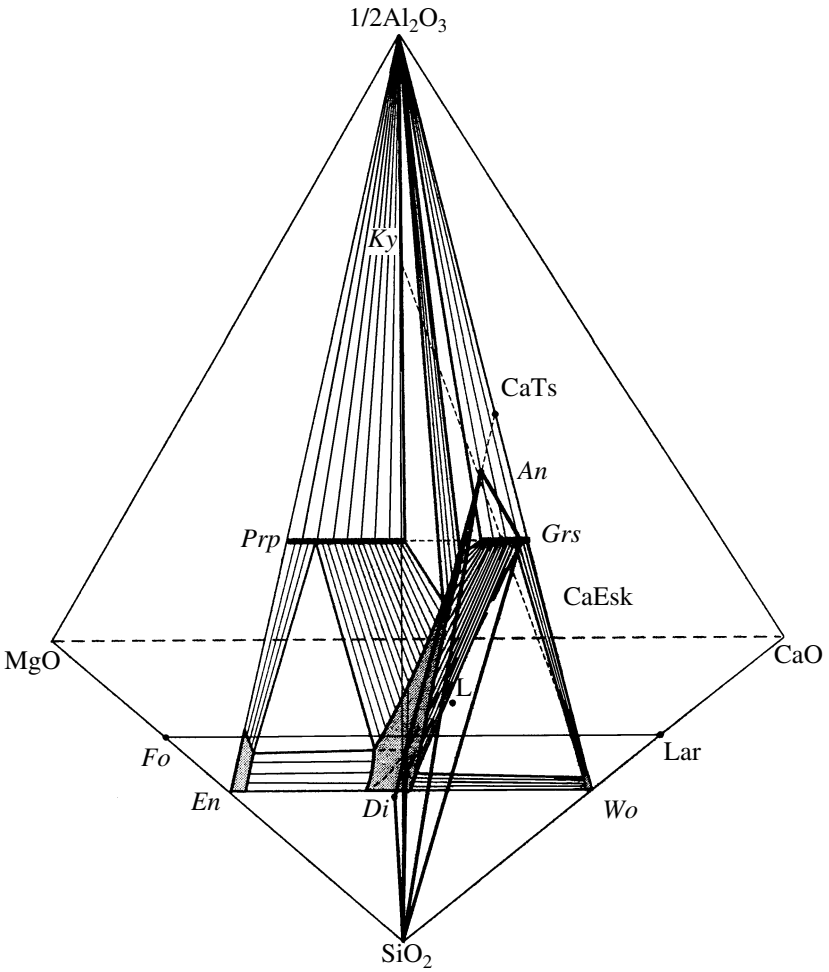

Fig. 1. Phase relations in the CaO–MgO–Al_2O_3–SiO_2 system at a pressure of 3.0 GPa. Phase relations in the plane $Mg_2Si_2O_6$–Al_2O_3–$Ca_2Si_2O_6$ are shown for a temperature of 1200°C according to the data of Boyd [29].

At a pressure of 2.0 GPa, nonstoichiometric clinopyroxenes coexist with anorthite, quartz, and α-diopside in the subsolidus region. Melting is observed between 1200 and 1300°C. The composition of liquid is enriched in calcium and approaches the subsystem CaO–Al_2O_3–SiO_2. Melting at a pressure of 2.0 GPa occurs via the eutectic reaction $\alpha Di + Cpx + An + Qtz = L$

Thus, the assemblage of nonstoichiometric clinopyroxene changes with decreasing pressure from a garnet-bearing to anorthite-bearing one. Such a change in phase assemblages is in good agreement with the results of previous work [13].

This implies that the invariant equilibrium (*L*, *An*, *Cpx*, *Grt*, α*Di*, *Qtz*) exists at a pressure between 2.0 and 3.0 GPa. The following univariant reactions emanate from the invariant equilibrium point:

$$(L)\ An + \alpha Di = Cpx + Grt + Qtz$$

$$(An)\ L = Cpx + Grt + \alpha Di + Qtz$$

$$\text{a) } (Cpx)\ L + Grt + Qtz = \text{An} + \alpha Di$$

$$\text{or b) } (Cpx)\ L + Grt = \text{An} + \alpha Di + Qtz$$

$$(Gr)\ L = An + Cpx + \alpha Di + Qtz$$

$$(\alpha Di)\ L + An = Cpx + Grt + Qtz$$

$$\text{a) } (Qtz)\ L + Grt = An + Cpx + \alpha Di$$

$$\text{or b) } (Qtz)\ L + Grt + Cpx = An + \alpha Di$$

Variants (a) of the clinopyroxene-free and quartz-free equilibria correspond to the case when the composition of liquid is more calcic than the *An*-α*Di*-*Qtz* plane. Variants (b) correspond to the case when the composition of liquid is more magnesian than the *An*-α*Di*-*Qtz* plane. The analyses of glasses from the 2.0 and 3.0 GPa experiments fall within the field of calcic compositions. Therefore, the former variants are realized and shown in Fig. 4.

A comparison of our results with the data of previous studies is complicated by the fact that the experimental studies were performed within different pressure–temperature regions. Nonetheless, the established features of the topological structure of the join either coincide or do not contradict the results of particular

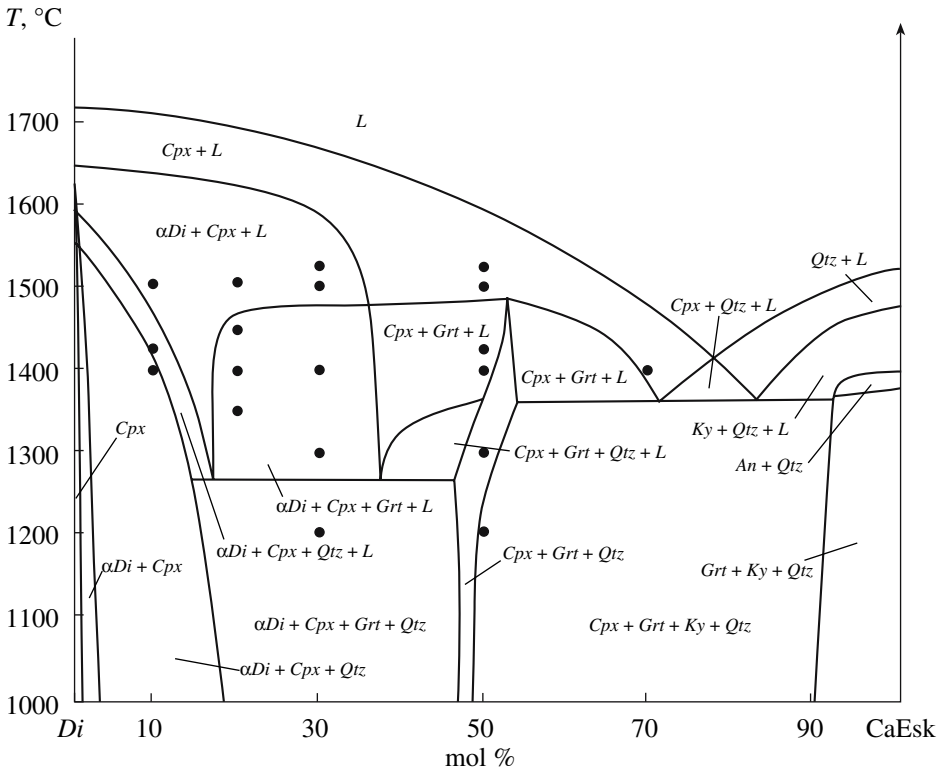

Fig. 2. Phase diagram for the join Di–CaEsk at a pressure of 3.0 GPa. The filled circles show the conditions of our experiments.

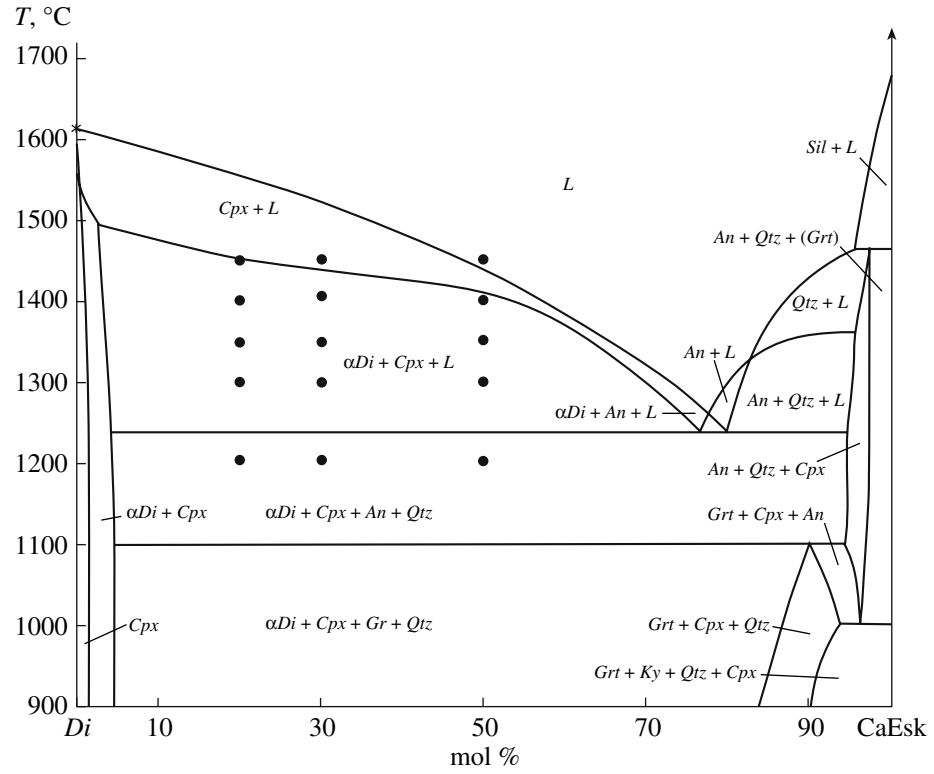

Fig. 3. Phase diagram of the join Di–CaEsk at a pressure of 2.0 GPa. The filled circles show the conditions of our experiments.

experiments from previous studies, although the interpretations of these results are significantly different.

In particular, the presence of the *Cpx + Grt + Ky + Qtz* assemblage in the calcic part of the system established by our experiments is in agreement with the experiments of [7–10], which established the phase fields *Cpx + Grt + Co* and *Cpx + Grt + Co + Ky* at a higher pressure of 3.5 GPa and a temperature of 1200°C. The existence of nonstoichiometric clinopyroxene–anorthite assemblages at a pressure of 2.0 GPa is consistent with the results of lower pressure experiments [12–13]. It should also be noted that the formation of clinopyroxene–anorthite assemblages at pressures of higher than 3.0 GPa, which was reported in some studies [18], is in conflict with the data on anorthite stability [30] and can be explained only by the influence of lead oxide, which was used as a flux in the Gasparik [18] experiments.

The experimental investigations reported here suggest that phase relations in the join diopside–Ca-Eskola component are more complicated than could have been supposed from the interpolation of the data of previous studies. The appearance of α-diopside results in the formation of the divariant assemblages (*An*, *Cpx*, α*Di*, *Qtz*) and (*Cpx*, *Grt*, α*Di*, *Qtz*). Furthermore, in addition to the previously known eutectic reaction *Cpx + Grt + Ky + Qtz = L*, melting occurs also via the reactions *L = An + Cpx + αDi + Qtz* and *L = Cpx + Grt + αDi + Qtz* at temperatures of 1200–1250°C. The compositions of liquid in these eutectic points are enriched in silica and calcium. Nonstoichiometric clinopyroxenes form complex solid solutions, the compositions of which are not strictly confined to the join under investigation and can be described in terms of four components, $CaMgSi_2O_6$, $CaAl_2SiO_6$, $Mg_2Si_2O_6$, and $Ca_{0.5}AlSi_2O_6$. The compositions of these solid solutions are controlled not only by pressure and temperature but also by the phase assemblage. Calcium-rich garnets coexist with nonstoichiometric clinopyroxene and α-diopside.

Taking into account the complex character of variations in the concentration of the Ca-Eskola component in clinopyroxene, the development of any geothermobarometric expression must account for the phase assemblage of nonstoichiometric clinopyroxene.

The identification of α-diopside in natural samples poses considerable difficulties because the prolonged cooling of a magmatic body can eradicate all evidence of the presence of this phase, including traces of twinning.

The unusually low melting temperatures in the eutectic reactions *L = An + Cpx + αDi + Qtz* and *L = Cpx + Grt + αDi + Qtz* may be of special importance for magmatic petrology. The compositions of melts in these eutectics are enriched in calcium and aluminum. Although the compositional volume within which melting occurs via these eutectic reaction is very narrow with respect to calcium and magnesium proportions, it overlaps the fields of basic, intermediate, and

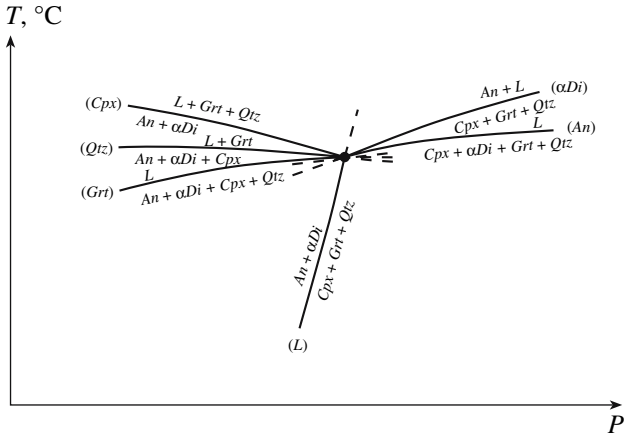

Fig. 4. Univariant equilibria emanating from the invariant equilibrium point (*L*, *An*, *Cpx*, *Grt*, α*Di*, *Qtz*).

felsic rocks. These reactions allow us to consider previously unknown evolution paths of magmatic melts and explain the accumulation of large volumes of these melts in magma chambers located within relatively cold lithospheric levels. The possibility of such a mechanism of the accumulation of large melt volumes must be taken into account in the analysis of the genesis of anorthosites and flood basalts.

In addition to the phase assemblages of corundum and quartz (coesite) kyanite eclogites and grospydites, the established phase relations revealed the phase volume of α-diopside assemblage, e.g., (α-*Di*)+*Cpx + Qtz + Grt,* the analogs of which were not yet found in rocks. The recognition of such associations as possible assemblages in the lower parts of the Earth's crust and in the upper mantle is very important for their subsequent identification among rocks and deep-seated xenoliths.

CONCLUSIONS

(1) Phase relations were investigated in the join diopside–Ca-Eskola component. Internally consistent phase diagrams were constructed for the join diopside–Ca-Eskola component at pressures of 2.0 and 3.0 GPa.

(2) The existence of an independent phase (α-diopside) whose composition approaches that of diopside was supposed on the basis of the experimental data. This phase becomes unstable with decreasing temperature and pressure and experiences a phase transformation to diopside, which is its closest compositional analog. The α-diopside phase forms a series of assemblages with nonstoichiometric clinopyroxene, garnet, anorthite, and quartz.

(3) An increase in pressure is accompanied by a change from anorthite-bearing to garnet-bearing assemblages of nonstoichiometric clinopyroxene. Grossular-rich garnet occurs in these assemblages. The invariant equilibrium (*L*, *An*, *Cpx*, *Grt*, α*Di*, *Qtz*) lies

within the pressure range 2.0–3.0 GPa. Nonstoichiometric clinopyroxene forms solid solutions with up to 20 mol % of the Ca-Eskola component.

(4) The hypothesis on the existence of α-diopside allowed us to explain low melting temperatures in the join diopside–Ca-Eskola molecule by the occurrence of a new type of eutectic reactions involving α-diopside.

ACKNOWLEDGMENTS

This study was financially supported by the Russian Foundation for Basic Research (project no. 05-05-64556), grant RNP.2.1.1.701 of the Ministry of Education of the Russian Federation, and the thematic program "The Development of the Potential of High School in 2006–2008."

REFERENCES

1. N. V. Sobolev, *Deep-Seated Inclusions in Kimberlites and the Problem of the Composition of the Upper Mantle*, Ed. by V. S. Sobolev (Nauka, Novosibirsk, 1974; Am. Geophys. Union, Washington, DC, 1977).
2. P. Eskola, "On the Eclogites of Norway," Videnskaps Skr. J., Kristiania, i mat. Nat. kl. **8**, 163–170 (1921).
3. I. Kushiro, "Clinopyroxene Solid Solutions Formed by Reactions between Diopside and Plagioclase at High Pressures," Mineral. Soc. Am. Spec. Pap. **2**, 179–191 (1969).
4. H. K. Mao, "The System Jadeite($NaAlSi_2O_6$)–Anorthite at High Pressure," Carnegie Inst. Wash. Yearbook **70**, 163–170 (1971).
5. V. A. Zharikov, I. P. Ivanov, Yu. A. Litvin, and R. A. Ishbulatov, "Experimental Study of the Melting of Calc-Alkaline Igneous Rocks at 35 Kbar," Dokl. Akad. Nauk SSSR **219**, 443–446 (1974).
6. R. A. Ishbulatov, "Experimental Study of the Calc-Alkaline Series at 25–45 kbar," in *Contributions to Physicochemical Petrology* (Nauka, Moscow, 1977), No. 6, pp. 97–167 [in Russian].
7. L. T. Khanukhova, V. A. Zharikov, R. A. Ishbulatov, and Yu. A. Litvin, "Excess Silica in High-Pressure Clinopyroxene Solid Solutions Based on Experimental Study of the System $CaMgSi_2O_6$–$CaAl_2SiO_6$–SiO_2 at 35 kbar and 1200°C," Dok. Akad. Nauk SSSR **229**, 182–184 (1976).
8. L. T. Khanukhova, V. A. Zharikov, R. A. Ishbulatov, and Yu. A. Litvin, "Pyroxene Solid Solutions in the System $NaAlSi_2O_6$–$CaAl_2SiO_6$–SiO_2 at 35 kbar and 1200°C," Dokl. Akad. Nauk SSSR **231**, 185 (1976).
9. L. T. Khanukhova, V. A. Zharikov, R. A. Ishbulatov, and Yu. A. Litvin, "The Silica Saturation Surface in the System $CaMgSi_2O_6$–$NaAlSi_2O_6$–$CaAl_2SiO_6$–SiO_2 at 35 kbar and 1200°C," Dokl. Akad. Nauk SSSR **234**, 168–171 (1977).
10. L. T. Khanukhova, "Experimental Study of the $CaMgSi_2O_6$–$NaAlSi_2O_6$–$CaAl_2SiO_6$–SiO_2 System at 35 kbar and 1200°C," in *Contributions to Physicochemical Petrology* (Nauka, Moscow, 1978), No. 8, pp. 155–178 [in Russian].
11. V. A. Zharikov, R. A. Ishbulatov, L. T. Chudinovskikh, and Yu. A. Litvin, "Solubility of $Ca_{0.5}AlSi_2O_6$ End Member in Clinopyroxenes and the Problem of the Eclogitic barrier," in *Proceedings of All-Russia Symposium on Mantle Xenoliths and Problems of Ultramafic Magmas, Novosibirsk, Russia, 1980* (Novosibirsk, 1980), p. 88 [in Russian].
12. R. A. Ishbulatov, L. T. Chudinovskikh, and E. K. Malinovskaya, "Experimental Study of Solubility of the $Ca_{0.5}AlSi_2O_6$ End Member in Clinopyroxenes at Pressure from 14 do 70 kbar," in *Proceedings of 13th Congress of International Mineralogical Association (IMA), Varna, Bulgaria, 1982* Ser. Bulg. Akad. Nauk. Crystallochem. Min., 351–357 (1986).
13. E. K. Malinovskaya, A. M. Doroshev, V. K. Bulatov, and G. Brey, "Clinopyroxenes of the $CaMgSi_2O_6$–$CaAl_2SiO_6$–$Ca_{0.5}AlSi_2O_6$ Series in Association with Anorthite, Quartz, Coesite, and Garnet," Geokhimiya, No. 2, 216–226 (1991).
14. B. J. Wood, "Mixing Properties of Tschermakitic Clinopyroxenes," Am. Mineral. **61**, 599–602 (1976).
15. B. J. Wood and C. M. B. Henderson, "Compositions and Unit-Cell Parameters of Synthetic Non-Stoichiometric Tschermakitic Clinopyroxenes," Am. Mineral. **63**, 66–72 (1978).
16. T. Gasparik and D. H. Lindsley, "Phase Equilibria at High Pressure of Pyroxenes Containing Monovalent and Trivalent Ions," Mineral. Soc. Am. Rev. **7**, 309–339 (1980).
17. T. Gasparik, "Experimental Study of Subsolidus Phase Relations and Mixing Properties of Pyroxene in the System CaO–Al_2O_3–SiO_2)," Geochim. Cosmochim. Acta **48**, 2537–2545 (1984).
18. T. Gasparik, "Experimental Study of Subsolidus Phase Relations and Mixing Properties of Clinopyroxene in the Silica-Saturated System CaO–MgO–Al_2O_3–SiO_2," Am. Mineral. **71**, 686–693 (1986).
19. N. V. Surkov, Yu. G. Gartvich, and Yu. V. Babich, "Experimental Study of the Phase Diagram of $CaMgSi_2O_6$–$CaAl_{0.5}Si_2O_6$ System at 3.0 GPa," Dokl. Akad. Nauk **398**, 533–537 (2004) [Dokl. Earth Sci. **398**, 1038–1042 (2004)].
20. F. R. Boyd and J. L. England, "Apparatus for Phase-Equilibrium Measurements at Pressures up to 50 Kilobars and Temperatures up to 1750°C," J. Geophys. Res. **65**, 741–748 (1960).
21. A. A. Godovikov, S. A. Smirnov, I. Yu. Malinovskii, et al., "Apparatus for Measurements at Pressures up to 40 kbar and Temperatures up to 1700°C," Prib. Tekhn. Eksp., No. 6, 159–160 (1971).
22. P. W. Mirwald, I. C. Getting, and G. C. Kennedy, "Low-Friction Cell for Piston–Cylinder High-Pressure Apparatus," J. Geophys. Res. **86**, 1519–1525 (1975).
23. N. V. Surkov, "A.s. SSSR. 1762458," Byull. Izobret. **34**, 213 (1992).
24. N. V. Surkov and G. N. Kuznetsov, "Experimental Study of the Stability of Clinopyroxene Solid Solutions in the Assemblage *Cpx*+ *Opx* + *Gr* in the CaO–MgO–Al_2O_3–SiO_2 System," Geol. Geofiz. **37** (12), 18–25 (1996).
25. A. M. Doroshev, I. Yu. Malinovskii, N. V. Surkov, and A. A. Kalinin, "Attainment of Equilibrium between Clinopyroxene and Garnets in the System CaO–MgO–Al_2O_3–SiO_2," in *Problems of Experiment in the High-Pressure Solid-Phase and Hydrothermal Appara-*

tuses," Ed. by I. I. Ivanov and Yu. A. Litvin (Nauka, Moscow, 1982) [in Russian].

26. A. M. Doroshev, N. V. Surkov, and I. Yu. Malinovskii, "Synthesis and Unit-Cell Parameters of Clinopyroxenes of the $CaMgSi_2O_6$–$Mg_2Si_2O_6$ Series," Zap. Vseross. Mineral. O-va, **110**, 629–632 (1981).
27. A. M. Doroshev, E. K. Malinovskaya, N. V. Surkov, and V. K. Bulatov, "Synthesis and Unit-Cell Parameters of Clinopyroxenes of the $CaMgSi_2O_6$–$CaAl_2SiO_6$ Series," Geokhimiya, No. 12, 1755–1764 (1986).
28. N. V. Surkov, "Stability of Aluminous Clinopyroxenes of the $CaMgSi_2O_6$–$CaAl_2SiO_6$ Series at High Pressures," in *Experimental Studies with Applications to the Problems of the Upper Mantle*, Ed. by A. A. Godovikov, A. M. Doroshev, and I. Yu. Malinovskii (IGiG, Novosibirsk, 1982), pp. 51–62 [in Russian].
29. F. R. Boyd and J. K. England, "Effect of Pressure on the Melting of Diopside, $CaMgSi_2O_6$, and Albite, $NaAlSi_3O_8$, in the Range up to 50 Kilobars," J. Geophys. Res. **68**, 311–323 (1963).
30. N. V. Surkov and A. M. Doroshev, "Phase Diagram of the CaO–Al_2O_3–SiO_2 System at Pressures up to 40 kbar," Geol. Geofiz. **39**, 1254–1268 (1998).